Interaction Notes

Note 529

July 3, 1997

A Comparison of Exact Versus Perturbed Pole Locations
of Dielectric Objects in Dielectric Medium

Mark C. Worthy
University of Alabama in Huntsville

Carl E. Baum
Phillips Laboratory

Abstract

The dielectric properties of soils and plastic targets are given. The approach for finding exact pole locations from a dielectric infinite slab, a dielectric sphere, and a dielectric infinite cylinder is presented (and applied). The exact poles for the slab and sphere are found for various sizes and dielectric properties. There is a discussion (and use) of Carl E. Baum's perturbation formulas for dielectric slabs and spheres. George Hanson's results (formulas, from using Carl's same approach) are given (and used) for an infinite dielectric cylinder. The poles found from the perturbation formulas are compared with the exact poles and an "effective" region for using the perturbation formulas is established.

19980602 002

$PL97-0944$

Contents

I. Introduction

The problem of finding buried UXO (unexploded ordnance) and dielectric mines has been well documented in recent years. According to the Department of Defense there are approximately nine million acres of past and present test ranges that contain ordnance [MMWG, 1996]. As a US citizen what is perhaps most disturbing is that there are between 1200 and 1700 Formerly Used Defense Sites (FUDS, now public or private land) which are believed to be contaminated [MMWG, 1996]. As for dielectric mines, war zone areas like Bosnia, Iraq, and Afghanistan have demonstrated just how lacking in technology we are in finding buried plastic targets.

As far as R&D funding goes we have reached a point where the government wants something that can tell the user whether or not the underground object that is being detected is in fact ordnance (and perhaps what type of ordnance it is) as opposed to just being an old soup can, plastic toy, or ordnance that has exploded and is now environmentally inert. Well if these things were in the air we might be able to do this; however, distinguishing objects underground can be an electromagnetic nightmare.

A common cry from the scientist and military personnel working on this project has been to establish a library of what the electromagnetic pole signatures of the various ordinance and mines look like. With such a library a user could know if what has been detected is of interest. Developing this library, however, is no simple task. In 1994 Carl E. Baum developed an approach for using perturbation formulas (much more condensed, yet approximate, mathematical formulas) to find the signatures of basic dielectric geometrical shapes in a dielectric medium [Baum, 1994]. It is the purpose of this report to establish the effectiveness of these formulas by comparing them to the exact cases. If their effectiveness is proven then the same approach could be used in creating our library.

II. Dielectric Properties of Soils and the Ordnance

Scattering of electromagnetic waves occur when there is a difference between the dielectric properties of the target and the medium [McCann et al., 1988]. Dielectric targets of interest in the ordnance and mine problem typically have a permittivity, ε, of about $2.5\,\varepsilon_o$. The earth, unfortunately, is not as predictable.

The dielectric properties of soil not only depend upon the type of soil but also the amount of moisture (and minerals) in the soil. For clays as the water content rises from 0 to 40% ε rises quickly from 3 to $\cong 20\,\varepsilon_o$ [Wang, 1978]. For sandy soils ε rises from 3 to $\cong 30\,\varepsilon_o$ [Wang, 1978]. The conductivity, σ, of the soils rises from $\cong .001$ to $\cong .1$ S/m for a rise in water content.

For the results found in the following pages I will use a target permittivity, ε_2, of $2.5\,\varepsilon_o$ and will look at soil permittivities, ε_1, ranging from 4 to $20\,\varepsilon_o$ and conductivity's, σ_1, ranging from .001 to 1 S/m. I will also look at the case where the target is in water $\varepsilon_1 = 81\,\varepsilon_o$ (and salt water $\varepsilon_1 = 81\,\varepsilon_o$, $\sigma_1 \cong 4$ S/m), as well as the case when $\varepsilon_1 >> \varepsilon_2$.

III. The Exact Approach

The signature differences of the scattered waves from a target not only depend upon these dielectric differences but also upon the various shapes and sizes of the targets. The scattered wave-forms for basic geometric shapes have been derived from many different physicist. The poles of these waves can be found by solving for the poles of the scattering coefficients. In the following section I will present these derived wave-forms and there coefficients for a dielectric sphere, infinite slab, and infinite cylinder.

Before I present these three cases, however, I should define a few important terms. The relative dielectric constant, ε_r, will be defined as

$$\varepsilon_r \equiv \frac{t \arg et}{medium} = \frac{\varepsilon_2}{\varepsilon_1}$$

The propagation constants for the medium, γ_1, and the target, γ_2, are

$$\gamma_1 = s\sqrt{\mu_o \varepsilon_1}\left[1 + \frac{\sigma_1}{s\varepsilon_1}\right]^{\frac{1}{2}}$$

and

$$\gamma_2 = s\sqrt{\mu_o \varepsilon_2}$$

where $s = \Omega + j\omega \equiv$ the complex frequency.

Finally, the ratios of these propagation constants, ξ, will be defined as

$$\xi \equiv \frac{\gamma_1}{\gamma_2} = \varepsilon_r^{-\frac{1}{2}}\left[1 + \frac{\sigma_1}{s\varepsilon_1}\right]^{\frac{1}{2}}$$

Sphere:

The series solution for a plane wave falling upon a sphere was first introduced by Mie in 1908. In 1941 Julius Adams Stratton provided a more extensive and complete model of the problem in his infamous book entitled Electromagnetic Theory. For derivations of the following equations I refer you to Stratton, 1941 or the Laplace form in Baum, 1992.

The scattered electric, E, and magnetic, H, waves from a dielectric sphere are

$$E_{sc} = E_o f(s)\sum_{n=1}^{\infty} (-1)^n \frac{2n+1}{n(n+1)}\left[-a_n M_{n,o}(\gamma_1 r) + b_n N_{n,e}(\gamma_1 r)\right]$$

$$H_{sc} \equiv \frac{\sigma_1 + s\varepsilon_1}{\gamma_1} E_o f(s)\sum_{n=1}^{\infty}(-1)^n \frac{2n+1}{n(n+1)}\left[b_n M_{n,e}(\gamma_1 r) + a_n N_{n,o}(\gamma_1 r)\right]$$

4

Where r is the radius of the sphere and a_n and b_n are the scattering coefficients. These scattering coefficients are functions of $\gamma_1 r$ and $\gamma_2 r$, and they depend upon Bessel functions. Where here I will be using the modified spherical Bessel functions:

$$k_n(x) = \frac{e^{-x}}{x} \sum_{p=0}^{n} \frac{(n+p)!}{p!(n-p)!} (2x)^{-p}$$

$$i_n(x) = \frac{1}{2}\left[-k_n(-x) + (-1)^{n+1} k_n(x)\right]$$

The scattering coefficients have been derived as

$$a_n = \frac{-\left[\frac{1}{\xi}\left[\gamma_2 r i_n(\gamma_2 r)\right]' i_n(\gamma_1 r) - \gamma_2 r i_n(\gamma_2 r)\frac{\left[\gamma_1 r i_n(\gamma_1 r)\right]'}{\gamma_1 r}\right]}{\left[\frac{1}{\xi}\left[\gamma_2 r i_n(\gamma_2 r)\right]' k_n(\gamma_1 r) - \gamma_2 r i_n(\gamma_2 r)\frac{\left[\gamma_1 r k_n(\gamma_1 r)\right]'}{\gamma_1 r}\right]}$$

$$b_n = \frac{-\left[\left[\gamma_2 r i_n(\gamma_2 r)\right]' i_n(\gamma_1 r) - \gamma_2 r i_n(\gamma_2 r)\frac{\left[\gamma_1 r i_n(\gamma_1 r)\right]'}{\xi\gamma_1 r}\right]}{\left[\left[\gamma_2 r i_n(\gamma_2 r)\right]' k_n(\gamma_1 r) - \gamma_2 r i_n(\gamma_2 r)\frac{\left[\gamma_1 r k_n(\gamma_1 r)\right]'}{\xi\gamma_1 r}\right]}$$

In solving for the poles of the scattered waves, a_n will correspond to the H-modes, and b_n will correspond to the E-modes. Therefore, the exact poles, s_α, of the H-modes for a dielectric sphere can be found from the equation

$$\frac{1}{\xi}\left[\gamma_2 r i_n(\gamma_2 r)\right]' k_n(\gamma_1 r) - \gamma_2 r i_n(\gamma_2 r)\frac{\left[\gamma_1 r k_n(\gamma_1 r)\right]'}{\gamma_1 r} = 0$$

and the exact poles of the E-modes for a dielectric sphere can be found from the equation

$$\left[\gamma_2 r i_n(\gamma_2 r)\right]' k_n(\gamma_1 r) - \gamma_2 r i_n(\gamma_2 r)\frac{\left[\gamma_1 r k_n(\gamma_1 r)\right]'}{\xi\gamma_1 r} = 0$$

Slab:

We will now consider the case of the infinite dielectric slab, with thickness l, in a dielectric medium. Technically there would not be natural frequencies since the pole locations depend upon the direction of the incident wave [Baum, 1994]. However, since we are really interested in finite size targets we will assume normal incidence. Making this assumption the scattering coefficient R_o, has been derived as [Baum, 1994]:

$$R_o = \frac{\left[\xi^2 - 1\right]\sinh(\gamma_2 l)}{2\xi \cosh(\gamma_2 l) + \left[\xi^2 + 1\right]\sinh(\gamma_2 l)}$$

Note that there is only one scattering coefficient here. This is because the magnetic field is polarized (parallel to the electric field, so the E and H poles are the same). This implies that the exact poles, s_α, for the dielectric slab can be found from the equation

$$2\xi\cosh(\gamma_2 l) + \left[\xi^2 + 1\right]\sinh(\gamma_2 l) = 0$$

Cylinder:

For the dielectric infinite cylinder the we do not have the spherical wave-forms that we had in the case of the sphere. Therefore, the Bessel functions in the scattering coefficients will be the standard first and second order Bessel functions (not spherical or modified spherical). These Bessel functions in the integral form are

$$J_n(x) = \frac{1}{\pi}\int_0^\pi \cos(x\sin\theta - n\theta)d\theta$$

and

$$H_n(x) = J_n(x) - iY_n(x)$$

where

$$Y_n(x) = \frac{1}{\pi}\int_0^\pi \sin(x\sin\theta - n\theta)d\theta - \frac{1}{\pi}\int_0^\infty \left[e^{n\phi} + (-1)^n e^{-n\phi}\right]e^{-x\sinh\phi}d\phi$$

The scattering coefficients a_n, and b_n derived in the ω form (s = jω) are [Balanis, 1989]

$$a_n = \frac{J_n'(\gamma_2 r)J_n(\gamma_1 r) - \xi J_n'(\gamma_1 r)J_n(\gamma_2 r)}{\xi J_n(\gamma_2 r)H_n'(\gamma_1 r) - J_n'(\gamma_2 r)H_n(\gamma_1 r)}$$

$$b_n = \frac{\xi J_n'(\gamma_2 r)J_n(\gamma_1 r) - J_n'(\gamma_1 r)J_n(\gamma_2 r)}{J_n(\gamma_2 r)H_n'(\gamma_1 r) - \xi J_n'(\gamma_2 r)H_n(\gamma_1 r)}$$

In the case of the dielectric cylinder the a_n coefficient corresponds to the E-modes and the b_n coefficient corresponds to the H-modes. Therefore, the exact poles, ω_α ($s_\alpha = j\omega_\alpha$), for the infinite dielectric cylinder can be found by

$$\xi J_n(\gamma_2 r)H_n'(\gamma_1 r) - J_n'(\gamma_2 r)H_n(\gamma_1 r) = 0$$

for the E-modes and

$$J_n(\gamma_2 r)H_n'(\gamma_1 r) - \xi J_n'(\gamma_2 r)H_n(\gamma_1 r) = 0$$

for the H-modes.

IV. Perturbation Formulas

To the casual observer these exact formulas probably don't look so bad. However, anyone who has ever had to expand Bessel functions will tell you that finding the poles of functions that contain multiples and derivatives (and multiples of derivatives) of Bessel functions would be a

cumbersome task. Recall also that these exact formulas are for nice geometrically shaped objects. Pole functions for real ordnance cases would be even more busy (much more). With this in mind Carl E. Baum made some approximations that would make these functions easier to work with for the slab and the sphere. The hope is that these perturbation functions will give results so close to the exact functions that others will be able to apply similar approximations to the exact pole functions for the real ordnance cases. The following paragraphs will show Baum's results for the slab and the sphere from his July 24, 1994 interaction note (IN 504).

Slab:

For the slab we will define the natural frequencies as
$$s_\alpha = s_{\alpha,0} + \Delta s_\alpha$$
where $s_{\alpha,0}$ is found from the limiting case when $\xi \to \infty$ giving
$$\sinh(s_{\alpha,0}\sqrt{\mu_o \varepsilon_2}\, l) = 0$$
note that this number will be imaginary. For Δs_α I refer you to Baum's work where

$$\Delta s_\alpha \approx -\frac{2\varepsilon_r^{\frac{1}{2}}}{\sqrt{\mu_o \varepsilon_2}\, l}\left[1 + \frac{i}{2}\frac{\sigma_1}{s_{\alpha,0}\varepsilon_1}\right]$$

Sphere:

The same method applied to the sphere has similar results where the poles are still
$$s_\alpha = s_{\alpha,0} + \Delta s_\alpha$$
Now, however, we will have different $s_{\alpha,0}$; one for the H-modes and one for the E-modes. For the H-modes as $\xi \to \infty$ we see that the exact formulas can reduce to
$$i_n(\gamma_2 r) = 0, \text{ or in other words: } i_n(s_{\alpha,0}\sqrt{\mu_o \varepsilon_2}\, r) = 0,$$
For the E-modes as $\xi \to \infty$ we can see that the exact formulas can reduce to

$$\left[\gamma_2 r i_n(\gamma_2 r)\right]' = 0, \text{ or in other words: } \left[s_{\alpha,0}\sqrt{\mu_o \varepsilon_2}\, r i_n(s_{\alpha,0}\sqrt{\mu_o \varepsilon_2}\, r)\right]' = 0$$

Again, $s_{\alpha,0}$ is a purely imaginary number. The Δs_α term for the sphere is nearly identical to the slab where

$$\Delta s_\alpha \approx -\frac{\varepsilon_r^{\frac{1}{2}}}{\sqrt{\mu_o \varepsilon_2}\, r}\left[1 + \frac{i}{2}\frac{\sigma_1}{s_{\alpha,0}\varepsilon_1}\right]$$

for the H-modes and

$$\Delta s_\alpha \approx -\frac{\varepsilon_r^{\frac{1}{2}}}{\sqrt{\mu_o \varepsilon_2}\, r}\left[1 + \frac{i}{2}\frac{\sigma_1}{s_{\alpha,0}\varepsilon_1}\right]\frac{(s_{\alpha,0}\sqrt{\mu_o \varepsilon_2}\, r)^2}{(s_{\alpha,0}\sqrt{\mu_o \varepsilon_2}\, r)^2 + n(n+1)}$$

for the E-modes.

Cylinder:

A fellow SRP worker (for RDL) George Hanson used Carl's same approach for an infinite dielectric cylinder. The results again, were very similar. Where $s_{\alpha,o} = j\omega_{\alpha,o}$, for the E-modes $s_{\alpha,0}$ can be found from $J_n(\gamma_2 r) = 0$, or in other words: $J_n(\omega_{\alpha,0}\sqrt{\mu_o\varepsilon_2}r) = 0$, and for the H-modes $s_{\alpha,0}$ can be found from $J_n'(\gamma_2 r) = 0$, or in other words: $J_n'(\omega_{\alpha,0}\sqrt{\mu_o\varepsilon_2}r) = 0$. For Δs_α George found

$$\Delta s_\alpha \approx \frac{-\varepsilon_r^{\frac{1}{2}}}{\sqrt{\mu_o\varepsilon_2}r}\left[1 + \frac{i}{2}\frac{\sigma_1}{s_{\alpha,0}\varepsilon_1}\right]$$

for the E-modes, and

$$\Delta s_\alpha \approx \frac{-\varepsilon_r^{\frac{1}{2}}}{\sqrt{\mu_o\varepsilon_2}r}\left[1 + \frac{i}{2}\frac{\sigma_1}{s_{\alpha,0}\varepsilon_1}\right]\frac{(s_{\alpha,0}\sqrt{\mu_o\varepsilon_2}r)^2}{(s_{\alpha,0}\sqrt{\mu_o\varepsilon_2}r)^2 - n^2}$$

for the H-modes.

V. The Results

The results were found with great assistance from the Mathcad 6.0 Plus software using the root finder function. However, in order to find the exact (and perturbed) function's poles for the first three E-modes and H-modes the functions had to be greatly simplified before they could be put into Mathcad. This meant analytically expanding, multiplying, and taking the derivatives of the first three Bessel, Hankle, modified spherical Bessel, and modified spherical Hankle functions (then reducing them). Reducing them was a tedious but necessary task (Mathcad's root finder wouldn't work with the functions in their expanded form). The root finder itself uses the secant method (similar to the Newton method). It was still necessary to make some adjustments to the software before it would work, and anyone who has ever used this root finder knows that it is highly dependent on initial guesses.

In the case of the cylinder I was unable to find the "exact" poles. The problem revolved around the standard Newman functions (and their derivatives). The software could calculate values for the exact functions, but to set them equal to zero to find the roots would cause the software to lock up. I had to truncate part of the integration involved in the Newman functions in order to get results. Therefore, what poles were found for the dielectric cylinder were not "exact." These poles did, however, provide a "check" for the poles from the perturbation formulas. Note that I could find poles from the perturbation formulas for the cylinder but not from the exact formulas (hence, the perturbation formulas are already proving their usefulness).

In order to show all of my results for this project I would need the paper equivalent to that used in making War and Peace. Therefore, I will instead list all of the cases that I found poles for and present a graph that shows the most effective regions for the perturbed functions.

8

The following is a list of the 42 different cases that poles were found for both the exact and the perturbed functions for the dielectric slab and sphere.

| $\varepsilon_1/\varepsilon_o$	σ_1	$\varepsilon_2/\varepsilon_o$	r, L
4	0, .01, .1	2.5	10cm
5	0, .01, .1	2.5	10cm
5	0, .01, .1	2.5	50cm
6.25	.094,.15	2.5	10cm
10	0,.001,.01,.1,.17	2.5	10cm
10	.2,.235,.27,.3	2.5	10cm
10	0, .01, .1	2.5	50cm
20	0,.01,.1,.2,.3,.4	2.5	10cm
81	0,.01,.1,1.36,2.6,4	2.5	10cm
1E+09	0, .1, 1.0	1	10cm
1.00E+09	1.0E+07	1	10cm
1E+09	1.5E+09	1	10cm
1E+09	2.1E+09	1	10cm

Condensing all 42 different cases into a graph that would establish an effective region for the perturbation functions required two jobs. First I found the percent errors for all 42 cases between the exact versus perturbed poles. Then I established two unit-less parameters, τ and ε_r, for

graphing. Where:
$$\tau = \frac{r\sigma_1\sqrt{\mu_o\varepsilon_2}}{\varepsilon_1} \quad \text{and} \quad \varepsilon_r = \frac{\varepsilon_2}{\varepsilon_1}$$
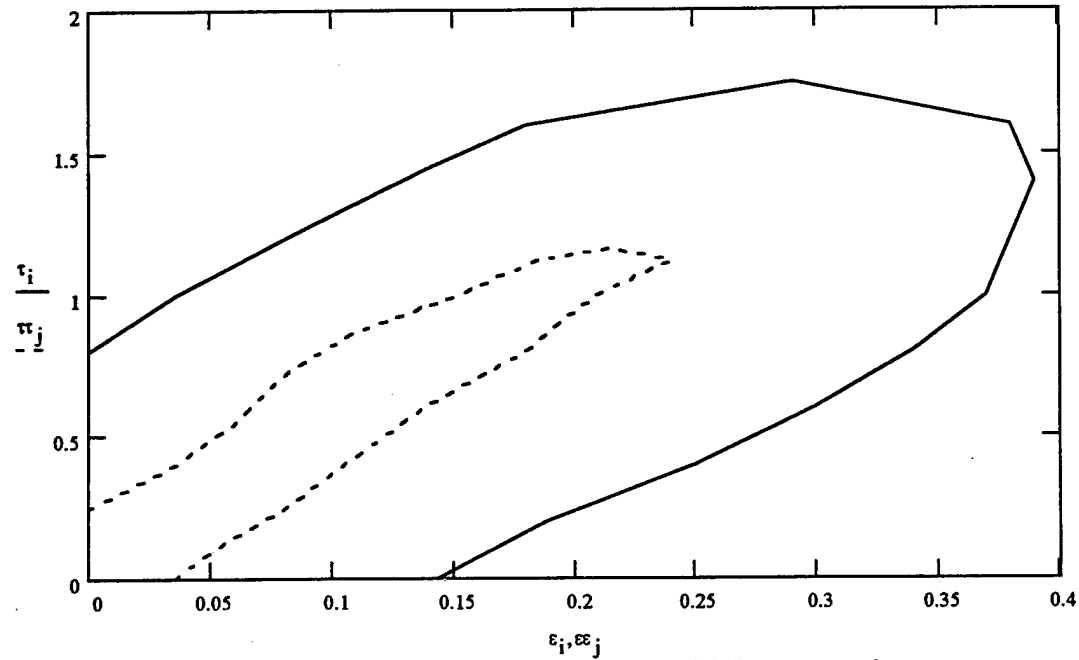
In the following graphs everything inside the curves represents a "good" region. In the first graph the poles from the perturbed functions were less than 6% off for the region inside the curve, and in the second graph (next page) the poles from the perturbed functions were less than 2% off.
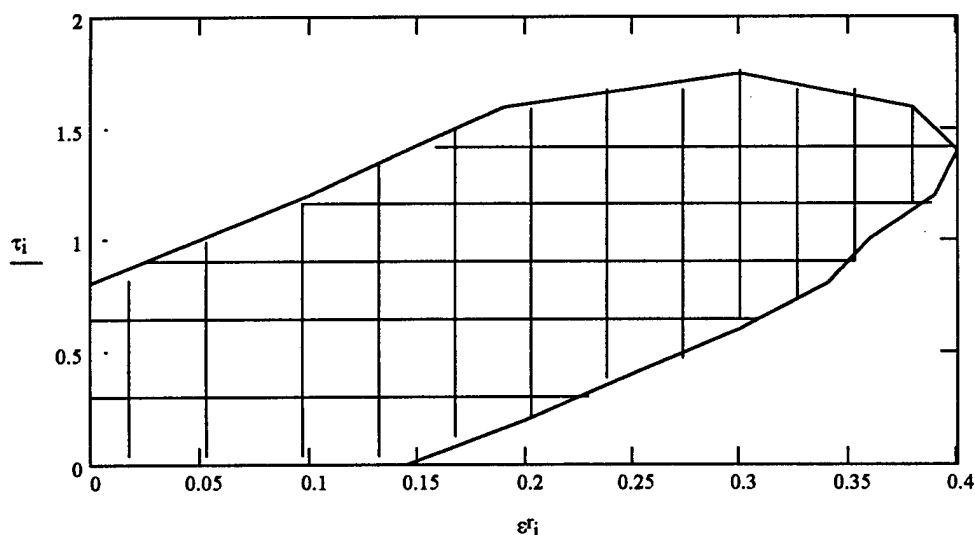
Graph 1: < 6% error for perturbed functions
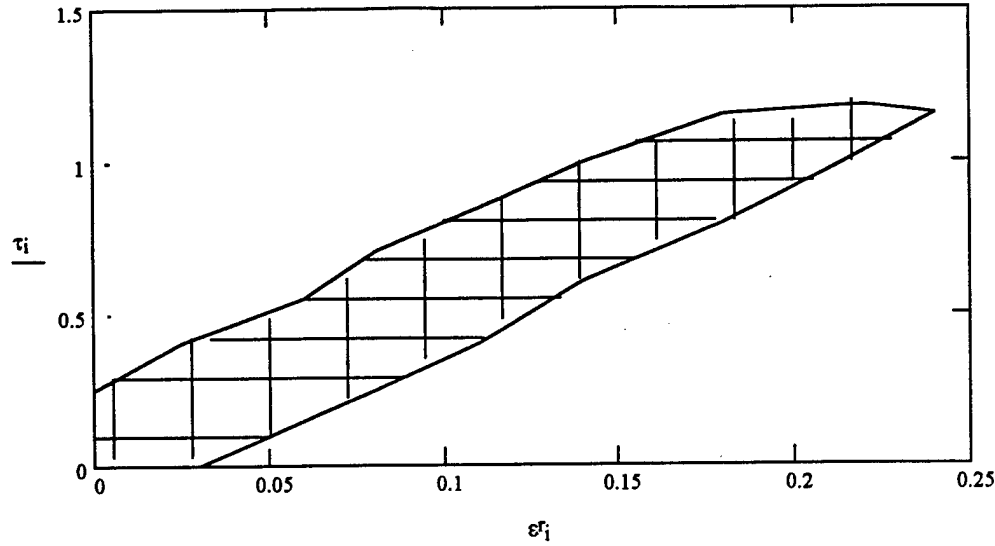
Graph 2: < 2% error for perturbed functions

Graph 3: An overlay of the 2% and 6% error graphs

VI. Discussion

The first point that I would like to make is about the nature of the poles themselves (exact or perturbed). The closer ε_1 gets to ε_2 the more shift to the left for the real components (with very little change in the imaginary terms). I should also point out that for the exact poles there was a non complex pole that doesn't show up using the perturbed functions. However, since real roots don't oscillate they wouldn't show up on radar anyway. I did notice, as theory dictates, a "layering" effect for the poles of the sphere and slab.

10

The effect of the conductivity term, σ_1, is

Sphere/Slab Poles for σ_1=0   Sphere/Slab Poles for increasing σ_1
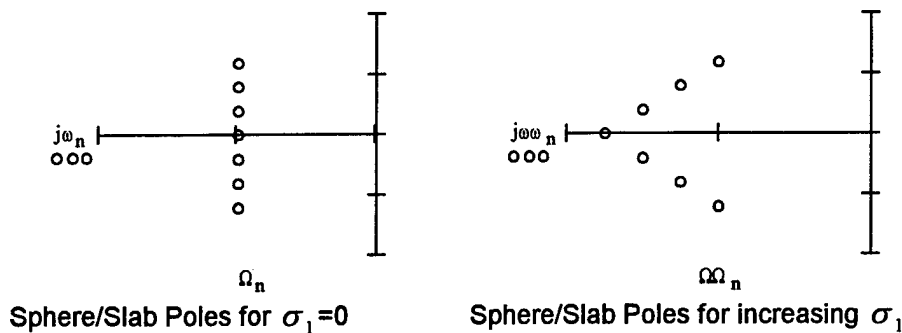
The greater the conductivity of the soil the more acutely angled shaped the pole-layer became. Where the perturbation formulas usually had greatest errors for the most damped of those poles (poles that were furthest left).

As for the size of the target usually being 10cm, generating poles for other size targets would simply involve the following: if the target is increased in size by some factor, k, then the poles would be decreased by this same factor and vice-versa (for σ_1=0; this is only an approximation for other σ_1).

For cases where $\varepsilon_1 >> \varepsilon_2$ increasing ε_1 by a factor of 100 decreased the real part of the poles by a factor of 10 (for ε_2=1). The imaginary term remained the same.

There were some unexpected results in comparing the poles for the exact versus perturbed functions. Notice from the graphs (in the result section) that there are many cases where some εr would contain "good" values but for σ_1=0 (τ=0) the percent errors were to large to be considered "good." I noticed when compiling the percent errors that as σ_1 is increased (hence, as τ is increased) the error decreased until it reached some minimum, then the error would begin to increase until it was too large to be considered "good." This explains the reason for the similar shapes of the two graphs ("<6% error," versus "<2% error").

The effectiveness region established for the perturbation functions would be applicable to many different soils. Where for soils (with plastic targets) τ ranges between 0 and 1 and ε_r ranges between 0.1 and 0.6. The "<6% error" graph shows "good" results for τ ranging (nonlinearly) from 0 to 1.75 and ε_r ranging (nonlinearly) from 0 to 0.4. The **best** results from the perturbed functions correspond to low-moisture soils.

In comparing the poles from the perturbed formulas for the cylinder with the poles from the "near" exact formulas I was able to get low percent errors. In fact the results seemed to show basically the same effectiveness region that was found for the sphere and slab case. However, since I was unable to get the "exact" poles (due to the computer limitations discussed earlier) I will not be presenting these results.

11

VII. Conclusions

The exact approach for finding the natural signatures for a dielectric sphere, and an infinite dielectric slab and cylinder were presented. This approach was used to find these poles for various size targets and different dielectric mediums.

An approximate approach for finding these same results was presented. The results found from these approximation formulas were compared to the exact poles. A region of effectiveness was established for these approximating formulas. This region varied with for τ ranging (nonlinearly) from 0 to 1.75 and ε_r ranging (nonlinearly) from 0 to 0.4. The effective region theoretically contains many different types of soils. The approximation formulas showed the best results for low-moisture soils.

The approximation formulas proved their usefulness when the "exact" poles could not be found for a dielectric infinite cylinder. Although, "nearly" exact poles for the cylinder showed that the effectiveness region is close to that of the dielectric slab and sphere.

With these three very different shapes having basically the same effectiveness region, I feel fairly confident that this effectiveness region will be the same for any of the specific buried plastic ordnance cases. Therefore, the approximation approach made by Carl E. Baum will be of great assistance in developing a library of the natural frequencies of different plastic ordnance.

References

Balanis, C.A., Advanced Engineering Electromagnetics, John Wiley and Sons, Inc., New York, 1989.

Baum, C.E., Concerning the identification of buried dielectric targets, Phillips Laboratory's Interaction Note 504, July, 1994.

Baum, C.E., Representation of surface current density and far scattering in EEM and SEM with entire functions, Phillips Laboratory's Interaction Note 486, February, 1992.

Federal Advisory Committee To Develop On-Site Innovative Technologies (unauthored), Military Munitions Working Group - final report, Western Governors Association, Denver, CO, June, 1996.

McCann, D.M., P.D. Jackson, and P.J. Fenning, Comparison of the seismic and ground probing radar methods in geological surveying, Proc. IEE, 135(F-4), 380-389, 1988.

Stratton, J.A., Electromagnetic Theory, McGraw-Hill Book Company, New York, London, 1941.

Wang, J., T. Schmugge, and D. Williams, Dielectric constants of soils at microwave frequencies-II, NASA Technical Paper 1238; Goddard Space Flight Center; Greenbelt, Maryland; 1978.